A Selective, Inexpensive Probe for UV-Induced Damage in Nucleic Acids

Amira F. El-Yazbi and Glen R. Loppnow*

Department of Chemistry, University of Alberta, Edmonton, AB T6G 2G2, Canada

*To whom correspondence should be addressed:

(780) 492-9704 (phone), (780) 492-8231 (fax), glen.loppnow@ualberta.ca (e-mail)

Abstract

A Selective, Inexpensive Probe for UV-Induced Damage in Nucleic Acids

Amira El-Yazbi and Glen R. Loppnow*

Department of Chemistry, University of Alberta, Edmonton, AB T6G 2G2 CANADA

Absorption of UV light by nucleic acids can result in the formation of molecular lesions in DNA and RNA, leading to mutagenesis, carcinogenesis, and cell death. In this work, hairpin oligonucleotide probes, which have previously been shown to be selective for DNA damage, are used. The hypochromic effect, which arises from the formation of the target-hairpin hybrid when there is no damage, is used to measure the amount of UV damage by measuring the amount of single-stranded DNA oligonucleotides. With accumulated UV exposure, the target-hairpin hybrid concentration decreases and the absorbance increases, enabling detection of UV-induced DNA damage. Our results show that the selectivity for DNA damage of the hypochromism probe is comparable to the molecular beacon probes, detecting between one and three lesions in an oligonucleotide. In addition, this probe is more than ten times cheaper than molecular beacon probes. However, it shows lower sensitivity to DNA damage. This makes its use recommended for high-throughput, qualitative analysis of DNA damage. This introduces a simple, fast, mix-and-read assay for the detection of DNA damage.

Keywords

Hypochromism, DNA damage, Hairpin probe, Absorption spectroscopy.

1. Introduction

Absorption of solar UV radiation by DNA gives rise to photochemical products such as cyclobutane pyrimidine dimers (CPDs), [6-4] pyrimidine pyrimidinones, dewar pyrimidinones, and uracil and thymine photohydrates.[1-3] Other damage agents, such as oxidative conditions and ionizing radiation, lead to other DNA lesions, such as single- and double-strand breaks, 8-oxoguanosine and cross-links. All these damage products have been implicated in mutagenesis, carcinogenesis and cell death.[4-7]

The precise measurement of DNA damage is essential for understanding the lethal and mutagenic effects of UV-induced DNA photoproducts.[3] A number of techniques have been used to detect nucleic acid damage. These include gel electrophoresis,[8] capillary electrophoresis,[9,10] electrochemical,[9,11] HPLC,[12] mass spectrometric[13-15] and polymerase chain reaction (PCR) amplification[16] methods. While useful, these techniques are destructive and time-consuming. In addition, electrophoretic and chromatographic techniques need to isolate the probe–target hybrids from an excess of unhybridized probes, which include extra steps that may introduce additional lesions.[8]

Other spectroscopic techniques have recently been used to characterize nucleic acid damage. Typically, fluorescent methods offer enhanced sensitivity and the potential for use *in situ* or *in vivo*. Differences in the fluorescence lifetime of a dye intercalated in undamaged and damaged DNA have been used to detect DNA damage.[17] Fluorescently-labeled antibodies provide a highly selective probe of specific damage photoproducts, such as thymine cyclobutane pyrimidine photodimers.[18] More recently, molecular beacons (MBs) have been used for broad-spectrum

detection of DNA and RNA damage.[3,19,20] The inherent sensitivity of fluorescence makes the MBs sensitive probes of nucleic acid damage. However, despite the wide applications and the exquisite sensitivity and selectivity of MBs, they have some limitations.[21-26] For instance, MBs require site-specific labeling of each terminus of the hairpin with a fluorophore and a quencher, respectively. This dual labeling makes their synthesis and purification difficult and expensive.[21,22,24,26] Since the two termini of the hairpin are already occupied by the donor and acceptor, any further modification - for example, for attachment to a solid support - would require the incorporation of an additional modified nucleotide into the stem.[21,24] Furthermore, due to incomplete attachment of the quencher, some hairpins may only be labeled with the fluorophore. In this case, highly sensitive assays would be affected by a high background due to unquenchable probe molecules.[7,8] Finally, in the presence of a mixture of undamaged and damaged DNA, the MB hybridizes only with the undamaged target. Thus, the fluorescence intensity decreases with increasing amounts of damage, providing an inversely proportional signal to the amount of damage, i.e. negative detection of DNA damage.

The main focus of this work is to design an inexpensive alternative to MB probes, in which the produced signal is directly proportional to the amount of DNA damage (positive detection of DNA damage). We have previously reported a method for the positive detection of DNA damage using a 2-aminopurine (2AP) hairpin probe. [27] Using 2AP hairpins to detect damage offers high sensitivity and selectivity, and they have overcome most of the MB probe limitations. However, the 2AP hairpin probes are expensive, especially with an increasing number of 2AP nucleobases incorporated in the probe. In this paper, we will present a less expensive alternative for the positive detection of DNA damage based on a hybridization assay coupled with the hypochromic effect.

The hypochromic effect is a well known phenomenon in nucleic acids. [28,29] It is the lowering of the absorbance in the ultraviolet absorption spectrum which is associated with the better stacking of purine and pyrimidine residues in double-stranded oligonucleotides compared to single-stranded ones. Measurements of hypochromism have been used frequently to study the secondary structure of polynucleotides[30,31] and the stability of naturally occurring and synthetic DNA structures.[32] In this work, a detectable signal is obtained which increases directly with increasing DNA damage by using a hairpin probe (Scheme 1). The probe forms a hybrid with the undamaged target and the absorbance signal is significantly decreased. Because of the increased instability of the hybrid when damaged, the probe will preferentially dehybridize from the target and acquire the hairpin structure, increasing the concentration of single stranded damaged target and increasing the absorbance signal. Thus, the more damaged targets in the solution, the lower the number of double-stranded hybrids and the higher the absorbance signal.

The target oligonucleotide used in this study is dT_{17} because of its well-known photochemistry. In this target, CPD is the major photoproduct formed after UV-irradiation, with small amounts of the [6-4] pyrimidine pyrimidinone and the dewar pyrimidinone photoproducts.[1] Also, the 260 nm absorbance band of dT_{17} gradually bleaches with increasing irradiation time, indicating photoproduct formation and loss of the $C_5=C_6$ bond yielding an independent spectroscopic marker for DNA damage. Thus, the loss of the 260 nm absorbance band can be directly related to the concentration of the photoproducts formed. Furthermore, it has been reported that a tripyrimidine stretch represents a hot spot for UV-induced DNA damage.[34] To our knowledge, this study represents the first time DNA hypochromism is used to probe nucleic acid damage. The performance of the DNA hypochromism probe to detect UV-induced DNA damage was examined and compared to DNA MBs.

2. Experimental

2.1. Materials

The single-strand dT_{17} oligonucleotide target, the hypochromism hairpin probes and the MB probe (Scheme 1) were obtained from Integrated DNA Technologies Inc. (Coralville, Iowa) and purified by standard desalting. The MB was further purified with HPLC. The magnesium chloride ($MgCl_2$) and sodium chloride (NaCl) were obtained from EMD Chemicals Inc. (Gibbstown, New Jersey), Tris was obtained from ICN Biomedicals, (Aurora, Ohio) and ethylenediaminetetraacetic acid (EDTA) was obtained from BDH Inc. (Toronto, Ontario). All chemicals were used as received. Nanopure water from a Barnsted Nanopure (Boston, Massachusetts) system was used for all solutions. The oligonucleotide samples were each dissolved in nanopure water and kept frozen at −20 °C until needed.

2.2. UV-Irradiation

Nitrogen-purged solutions of 10 µM dT_{17} (20 mM Tris, 1 mM EDTA, 3 mM $MgCl_2$, 50 mM NaCl, pH 7.5) were irradiated in sealed, UV-transparent 1 cm path length cuvettes. The cuvettes were placed in a water bath also contained in a UV-transparent water dish. The temperature, which was monitored by means of a Cole-Parmer DiGi-SENSE thermocouple (Niles, Illinois), was kept constant throughout the irradiation by the water bath. Oligonucleotide samples were irradiated in a Luzchem (Ottawa, Ontario) DEV photoreactor chamber with UVC light from lamps emitting principally at 254 nm with a power density of 75 W m^{-2}. The samples were constantly stirred during irradiation, and the photoreactor was purged with nitrogen throughout the irradiation to flush out oxygen and any ozone subsequently generated from the UVC lamps.

Control samples were handled identically, but were not exposed to UV radiation. The UVC lamps were turned on ~20 min before the start of irradiation to stabilize the lamp output.

2.3. Absorbance *and fluorescence measurements*

Absorption spectra were recorded at intervals throughout the irradiation period on a Hewlett-Packard (Sunnyvale, California) 8452A diode array spectrophotometer by placing the irradiated cuvettes containing the target oligonucleotide solutions directly into the spectrophotometer. For the hypochromism measurements, a 20 µL aliquot of each irradiated solution was taken at various time intervals and was later mixed with an equimolar amount of the hypochromism hairpin probe. Then, buffer solution was added to have a total volume of 100 µL. The 260 nm absorption maxima were recorded for aliquots at different time intervals. For the fluorescence measurements, a 10 µL aliquot of each irradiated solution was taken at various time intervals and was later mixed with an appropriate amount of the MB probe and buffer solution to give final concentrations of 1 µM oligonucleotide target and 200 nM MB probe. These solutions were then incubated in the dark at room temperature for about 24 h. Fluorescence spectra of 100 µL aliquots of the incubated hybridization mixtures were measured using a Photon Technologies International (Birmingham, New Jersey) fluorescence system. The spectra were recorded between 500 and 700 nm with excitation at 490 nm. A 1 cm path length Suprasil quartz fluorescence cuvette was used for these measurements.

The hypochromism probe was characterized by a thermal denaturation profile experiment in which temperature-dependent absorbance measurements were carried out on a buffered 200 nM solution of the hairpin probe incubated in the presence of an equimolar amount of the target

oligonucleotide sequence. The temperature was varied from 20 to 72 °C in 4 °C increments at a heating rate of 1 °C min^{-1} and 5 min settling time for each step of the heating cycle.

3. Results and discussion

The hypochromism hairpin probe was carefully designed to maximize its performance as a sensitive and specific probe to UV-induced nucleic acid damage. Scheme 1 shows the structure of the hypochromism hairpin probe used in this study. The probe is designed such that the oligonucleotide target is complementary to the loop region and three nucleotides in the stem region to avoid sticky end pairing[33]. The design of the hypochromism probe maximizes discrimination of damaged *versus* undamaged targets, due to the T_m's of the stem and hybrid; designing the probe to have a T_m for the stem 5 – 10 °C higher than the T_m of the hybrid ensures maximum sensitivity.[19]

Figure 1 shows the effect of temperature and damage on the 260 nm absorbance of the oligonucleotide target-hairpin hybrid. The absorbance of the undamaged double-stranded hybrid is initially constant with increasing temperature. At temperatures close to the melting temperature of the hybrid, the absorbance starts to increase with increasing temperature as the hybrid melts. At temperatures greater than 60 °C, the absorbance is constant again at a maximum. These results suggest that the hybrid has melted at temperatures above 60 °C.

It is worth mentioning here that the trend shown in the thermal denaturation profile for the hypochromism hairpin probe in the presence of the target is different from the one expected from MB probes of damage.[3,19,20,33] At low temperatures, the fluorophore and the quencher in solutions containing the MB-target hybrid are far apart and maximum fluorescence is observed. At higher temperatures, the hybrid will melt and the MB will re-form the hairpin, leading to a

decrease in fluorescence. It is clear that the thermal denaturation profile of the hybrid of the target with the hypochromism probe shows an opposite trend to that with the MB probe and this is what allows the hypochromism signal to increase with increasing damage to the target.

Figure 1 also shows the absorbance as a function of temperature for a hybrid of the hypochromism hairpin probe and a UV-damaged oligonucleotide strand. Here, the hybrid between the hypochromism hairpin probe and the UV-damaged oligonucleotide target shows a higher absorbance than that of the hybrid between the hypochromism hairpin and the healthy target at low temperatures. In addition, the melting temperature of the damaged oligonucleotide hybrid (~42 °C) is less than the melting temperature of the undamaged oligonucleotide hybrid (~46 °C). As shown in Figure 1, there is good discrimination in the absorbance between the undamaged and damaged targets hybridized with the hypochromism probe at 20 $^{\circ}$C. Therefore, we have chosen this hybridization temperature for detecting the formation of the UV-induced photoproducts.

The dT_{17} oligonucleotide target was irradiated at constant temperature, and the resultant damage was detected by UV-Vis absorbance measurements of the irradiated and control samples. Figure 2 shows a plot of the absorbance of the oligonucleotide target as a function of irradiation time with UVC light. The 260 nm absorption band, which represents the $\pi\pi^*$ transitions of the nucleobases, is seen to decrease with time. This result is expected and indicates UV-induced damage to the oligonucleotides with the consequent loss of the $C_5=C_6$ bond in all photoproducts formed. This decrease in absorbance is not observed in the unirradiated controls, demonstrating that the absorbance changes arise from irradiation of the samples and subsequent photochemistry rather than any other effect.

In order to investigate the sensitivity and selectivity of the hypochromism probe to detect nucleic acid damage, we measured the absorbance of aliquots of the irradiated target samples after incubation for 24 hrs with the hairpin probe (Figure 3A). Aliquots of unirradiated samples of these solutions were also incubated with the probe as controls. It should be noted that the probe solution was not irradiated; it was only incubated with aliquots of irradiated oligonucleotide solutions, as well as their unirradiated controls. As shown in Figure 3A, the absorbance signal increases with UV irradiation and continues to increase with increasing irradiation until it reaches a plateau corresponding to the absorbance of the damaged target and unhybridized hairpin probe. This plateau is reached within the first 5 min of irradiation. This indicates that after 5 min irradiation, all of the hypochromism probes are in the hairpin form, and the solutions exhibit their maximum absorbance signal.

The plot of absorbance as a function of irradiation time for the oligonucleotide target (Figure 2) was fit to a double-exponential function while the hypochromism plot (Figure 3A) was fit to a single exponential growth function. For the absorbance (Figure 2), this decay represents the formation of thymine photoproducts containing saturated C_5-C_6 bonds and can be correlated to the concentration of the damage products. The increase in the absorbance signal in the hypochromism plot (Figure 3A) represents the decreased stability of the damaged target-hairpin hybrid. Therefore, the faster the absorbance signal increases, the more selective the probe is at detecting UV-induced oligonucleotide damage under identical irradiation conditions for the same target.

This method for the detection of UV-induced nucleic acid damage by the hypochromism probe was compared to the MB probe's ability to detect UV-induced damage. The MB probe (Scheme 1) used in this study was designed to the same sequence as the hypochromism probe. In addition,

a FAM fluorophore was attached to the 5'- end and a DABCYL quencher was attached to the 3'-end. As explained above, the fluorescence is quenched in the hairpin position when the FAM and DABCYL are in close proximity, and the fluorescence intensity is high in the presence of complementary target when the MB forms a hybrid with the target. As damage accumulates on the target strand, the MB-target hybrid becomes less stable, effectively decreasing the fluorescence intensity until the closed, hairpin form is the more stable form of the MB. This trend is shown in Figure 3B, in which the MB fluorescence intensity decreases with longer irradiation time until reaching a constant minimum corresponding to the fluorescence of the MB in the hairpin structure. The fluorescence curve was fit to a single exponential decay function. The damage constants obtained by the two probes are shown in Table 1 for the absorbance, MB and hypochromism probe methods for detecting DNA damage. The ideal probe would detect damage at the rate it is being formed, but the reality is that probes may not be sensitive to a single lesion. The damage constant reflects the instability of the damaged target-probe hybrid. The lower (faster) the damage constant, the more selective the probe is at detecting UV-induced DNA damage, to the limit of the target damage rate. It is clear from Table 1 that the rate of absorbance decay is slower than the rate of the increase of the absorbance in the hypochromism plot and the rate of decrease of the MB fluorescence. This indicates the lower selectivity of the absorbance measurements.[20] Table 1 also shows that the hypochromism hairpin probe has a lower damage constant than that of the MB probe, which indicates that it has a higher selectivity to detect DNA damage. This allows the hypochromism probe to have superior selectivity for detection of UV damage in nucleic acids compared to absorbance and the MB probe.

In order to check the sensitivity of the hypochromism probe for damage detection, we used the UV absorbance measurements as a function of UV irradiation time to quantify the amount of UV

damage and to develop calibration curves for the hypochromism probe. The procedure and calculation of the photoproduct concentrations from the absorbance of the irradiated solutions have been explained previously.[27] Figure 4 shows the calibration curve obtained upon plotting the hypochromism absorbance signal as a function of the total concentration of the photoproducts calculated for both the hypochromism and the fluorescence signal for the MB probes (Figure 4B). The signal at zero concentration of the photoproducts represents the background level corresponding to the highest hypochromism (least absorbance) of the probe when it is completely hybridized with the undamaged target. At photoproduct concentrations higher than 0.5 μM, the hybrid formed between the probe and the damaged strand is completely unstable, and the probe acquires the hairpin structure and is not hybridized with the damaged target giving maximum absorbance. Additional formation of photoproducts does not lead to any more unhybridization, so the absorbance signal shows saturation-like behaviour. For the DNA MB (Figure 4B), any decrease in fluorescence signal requires a minimum of 2.6 μM concentration of the photoproducts. The constant fluorescence signal of the DNA MB over the range of 0 – 2.6 μM of the photoproducts concentration can be attributed to the lower selectivity of the DNA MB to UV-induced DNA damage as discussed before. At high photoproduct concentrations, the hybrid formed between the DNA MB and the damaged strand is completely unstable, and the DNA MB preferentially acquires the hairpin structure where the fluorophore and the quencher are in close proximity and the fluorescence is the lowest. Any further damage doesn't lead to any additional decrease in fluorescence and the signal remains constant showing a saturation-like behaviour.

Table 2 shows the parameters for the quantification of UV-induced DNA damage from Figure 4. The calibration curve for the hypochromism probe shows a similar linear dynamic range to the MB

12

probe (Figure 4) taking into account the threshold response of 0.5 μM. On the other hand, the DNA MB requires concentrations of 2.6 μM or more to show any fluorescence response to the photoproducts formed. While the hypochromism probe has higher selectivity than the MB probe, the sensitivity of detection, calculated as the slope of the calibration curve (Figure 4), is 6 orders of magnitude higher for the MB probe than the hypochromism probe. This large difference in sensitivity can be attributed to the 6 order of magnitude difference between the fluorescence scale of the MB probe and the absorbance scale of the hypochromism probe. The MB probe has a limit of detection (LOD) and limit of quantitation (LOQ) lower by only 8 times than the hypochromism probe, though, since the LOD and LOQ correct for the higher deviations in the blank. These lower LOD and LOQ are due to the intrinsically higher sensitivity of the zero-background fluorescence detection. It is worth mentioning that the values recorded in Table 2 for the LOD and LOQ for the hypochromism probe and DNA MB detection of the UV-induced photoproducts are obtained by using the standard deviation of the blank measurements and the sensitivity of the method, while the LOD and LOQ will be practically limited to ~0.5 and ~2.6 μM, respectively (Figure 4B) due to the threshold shown at low photoproducts concentrations. From this data, upon multiplying the concentration of the irradiated DNA target by the number of nucleotides forming the DNA target and dividing by the LOD, we are able to calculate that the hypochromism probe can detect one damage site in the presence of ~260 undamaged sites, compared to one damage site in the presence of ~2060 undamaged site with the MB probe. This again confirms the higher sensitivity of the MB probe over the hypochromism probe.

These results conclusively show that the hypochromism probe has superior selectivity to detect UVC-induced oligonucleotide damage over the DNA MB. Although its sensitivity is not as good as

DNA MB probes, being 10 times cheaper than the DNA MB probes makes it an attractive tool for the high throughput qualitative analysis for UV-induced DNA damage.

4. Conclusion

In summary, the assay reported here uses the hypochromism phenomenon to design a probe for the detection of UVC-induced nucleic acid damage, by taking advantage of the hypochromic effect occurring in dsDNA. The hypochromism probe shows better selectivity for UVC-induced nucleic acid damage than MBs, but with lower sensitivity. Moreover, it is cheap, simple and easy to synthesize which introduces a new probe for the qualitative detection of UVC-induced DNA damage.

References

1. Ruzsicska, B. P.; Lemaire, D. G. E. in: Horspool, W. M.; Song, P.-S. (Eds.), DNA Photochemistry, CRC Handbook of Organic Photochemistry and Photobiology; CRC Press, New York. 1995, pp. 1289-1317.

2. Wagner, D. M.; Loppnow, G. R. *Spectrum* **2004**, 17, 26.

3. Yarasi, S.; McConachie, C. ; Loppnow, G. R. *Photochem. Photobiol.* **2005**, 81, 467.

4. Marrot, L.; Meunier, J. R. *J. Am. Acad. Dermatol.* **2008**, 58, S139.

5. Lindahl, T. *Nature* **1993**, 362, 709.

6. Marnett, L. J.; Burcham, P. C. *Chem. Res. Toxicol.* **1993**, 6, 771.

7. Ames, B. N.; Gold, L. S.; Willett, W. C. *Proc. Natl. Acad. Sci. USA* **1995**, 92, 5258.

8. Weinfeld, M.; Soderlind, K.-J. M. *Biochemistry* **1991**, 30, 1091.

9. Haab, B. B.; Mathies, R. A. *Anal. Chem.* **1995**, 67, 3253.

10. Le, X. C.; Xing, J. Z.; Lee, J.; Leadon, S.A.; Weinfeld, M. *Science* **1998**, 280, 1066.

11. Wang, J.; Rivas, G.; Ozsoz, M.; Grant, D. H.; Cai, X.; Parrado, C. *Anal. Chem.* **1997**, 69, 1457.

12. Kaur, H.; Halliwell, B. *Biochem. J.* **1996**, 318, 21.

13. Douki, T.; Court, M.; Sauvaigo, S., Odin, F.; Cadet, J. *J. Biol. Chem.* **2000**, 275, 11678.

14. Douki, T.; Cadet, J. *Biochemistry* **2001**, 40, 2495.

15. Ravanat, J.-L.; Douki, T.; Cadet, J. *J. Photochem. Photobiol. B: Biol.* **2001**, 63, 88.

16. Kumar, A.; Tyagi, M. B.; Jha, P. N. *Biochem. Biophys. Res. Commun.* **2004**, 318, 1025.

17. Trevithick-Sutton, C. C.; Mikelsons, L.; Filippenko, V.; Scaiano, J. C. *Photochem. Photobiol.* **2007**, 83, 556.

18. Xing, J. Z.; Lee, J.; Leadon, S. A.; Weinfeld, M.; Le, X. C. *Methods* **2000**, 22, 157.

19. El-Yazbi, A.; Loppnow, G. R. *Can. J. Chem.* **2011**, 89, 402.

20. Oladepo, S. A.; Loppnow, G. R. *Anal. Bioanal. Chem.* **2010**, 397, 2949.

21. Stohr, K.; Hafner, B.; Nolte, O.; Wolfrum, J.; Sauer, M.; Herten, D.-P. *Anal. Chem.* **2005**, 77, 7195.

22. Knemeyer, J.-P. ; Marme, N.; Sauer, M. *Anal. Chem.* **2000**, 72, 3717.

23. Misra, A.; Kumar, P.; Gupta, K. C. *Anal. Biochem.* **2007**, 364, 86.

24. Heinlein, T.; Knemeyer, J.-P.; Piestert, O.; Sauer, M. *J. Phys. Chem. B* **2003**, 107, 7957.

25. Kim, Y.; Yang, C. J.; Tan, W.H. *Nucl. Acids Res.* **2007**, 35, 7279.

26. Misra, A.; Shahid, M. *Bioorg. Med. Chem.* **2009**, 17, 5826.

27. El-Yazbi, A. F.; Loppnow, G. R. *Anal. Chim. Acta.* **2012,** 726, 44.

28. Rich, A.; Tinoco, I. *J. Am. Chem. Soc.* **1960,** 82, 6409.

29. Tinoco, I. *J. Am. Chem. Soc.* **1960**, 82, 4785.

30. Haschemeyer, R.; Singer B.; Fraenkel-Conrat, H. *Proc. Natl. Acad. Sci., USA.* **1959**, 45, 313.

31. Rich, A. *Nature* **1958**, 181, 521.

32. Hill, T. *J. Chem. Phys.* **1959**, 30, 383.

33. Yang, C. J.; Wang, L.; Wu, Y.; Kim, Y.; Medley, C. D.; Lin, H.; Tan, W. H. *Nucl. Acids Res.* **2007**, 35, 4030.

34. Weinfeld, M.; Liuzzi, M.; Paterson, M. C. *J. Biol. Chem.* **1989**, 264, 6364.

Table 1. Damage constants of the different DNA damage assay methods.

Method	Damage constant (min)[a]
Hypochromism Probe	$\tau = 1.02 \pm 0.02$
DNA MB fluorescence	$\tau = 3.59 \pm 0.2$
Absorbance	$\tau_1 = 6.08 \pm 0.07$
	$\tau_2 = 91.8 \pm 2.0$

[a]The damage constants (τ) were obtained from the fits in Figures 2 and 3.

Table 2. Analytical parameters for the quantification of UV-induced DNA damage with the hypochromism probe and DNA MB.

Parameter[a]	Hypochromism probe	DNA MB
Linear Dynamic Range	0.5 – 2.1 μM	2.60 – 4.50 μM
R^2	0.994	0.995
Sensitivity	2.9×10^5 M^{-1}	9.54×10^{11} cps M^{-1}
LOD	325.5 nM	41.4 nM
LOQ	1085 nM	138 nM

For the determination of the blank standard deviation, 20 solutions of the MB hairpin alone were used. The standard deviations of these measurements were 3.1×10^{-2} and 1.3×10^4 cps for the hypochromism hairpin probe and the DNA MB, respectively. [a]In this table, linear dynamic range is the concentration range corresponding to the linear region in the calibration curve, R^2 is the linear regression coefficient squared, sensitivity is the slope of the calibration curve, LOD is the limit of detection and is 3 times the standard deviation of the blank divided by the sensitivity, and LOQ is the limit of quantification and is 3.3 times the LOD.

Figure captions

Scheme 1. Sequences of the hypochromism hairpin and MB probes. "FAM" denotes the 6-carboxyfluorescein fluorophore, and "DABCYL" denotes the DABCYL quencher.

Figure 1. Thermal denaturation curves for 200 nM hypochromism hairpin probe in the presence of an equimolar amount of the perfectly complementary undamaged oligonucleotide target sequence (filled squares), and 200 nM hypochromism hairpin probe in the presence of an equimolar amount of the UV-irradiated oligonucleotide target sequence for 5 min (open squares) in 1 cm cuvettes. The lines are guides for the eye.

Figure 2. Absorbance of 10 μM irradiated target (filled squares) and unirradiated control (open squares) monitored at 260 nm as a function of irradiation time in 1 cm cuvettes. The solid line through the absorbance points (filled squares) is the least-squares fit to an offset, double exponential function, $A = A_0 + A_1e^{-t/\tau 1} + A_2e^{-t/\tau 2}$, where the absorbance damage constants are 6.08 ± 0.07 min (τ_1) and 91.8 ± 2.0 min (τ_2), and the amplitudes are $A_1 = 0.52 \pm 0.01$ and $A_2 = 0.66 \pm 0.02$. The offset (A_o) is 0.21 ± 0.02. The control points (open squares) are fit to a straight line with zero slope by eye.

Figure 3. Absorbance at 260 nm of the hypochromism hairpin probe (A) and fluorescence intensity at 520 nm of the DNA MB (B) as a function of irradiation time for the oligonucleotide targets (open squares) and unirradiated target controls (filled squares) in 1 cm cuvettes. Only the 10 μM target was irradiated. Aliquots of the irradiated target were mixed with equimolar amounts of both probes (10 mM Tris, 3 mM $MgCl_2$, 20 mM NaCl, 1 mM EDTA, pH 7.5). The solid line through the irradiated sample points (open squares) is a single exponential fit. The hypochromism probe absorbance (A) is fit by $A_t = A_0 + a (1 - e^{-t/\tau})$, where $A_0 = 1.3 \pm 0.01$, a =

0.58 ± 0.02, and τ = 1.02 ± 0.01 min. The MB fluorescence decay (B) is fit by $I_F = I_{F,0} + a\ e^{-t/\tau}$

where $I_{F,0}$ = 0.12 ± 0.04 × 10^6, and a = 2.5 ± 0.1 × 10^6, τ = 3.59 ± 0.2 min. The control points

(filled squares) are fit to straight lines of zero slopes by eye. Inset shows the absorbance at 260

nm of the hypochromism hairpin probe for the first 15 min of irradiation and the fluorescence

intensity at 520 nm of the DNA MB for the first 30 min of irradiation.

Figure 4. Calibration curve of DNA photodamage formed upon UV irradiation of the poly dT_{17}

target for the (A) hypochromism hairpin probe and (B) MB probe. Inset shows the fit to the

linear portions of the calibration curves. Each data point is an average of three replicate

measurements and the error bars correspond to the relative standard deviation of the

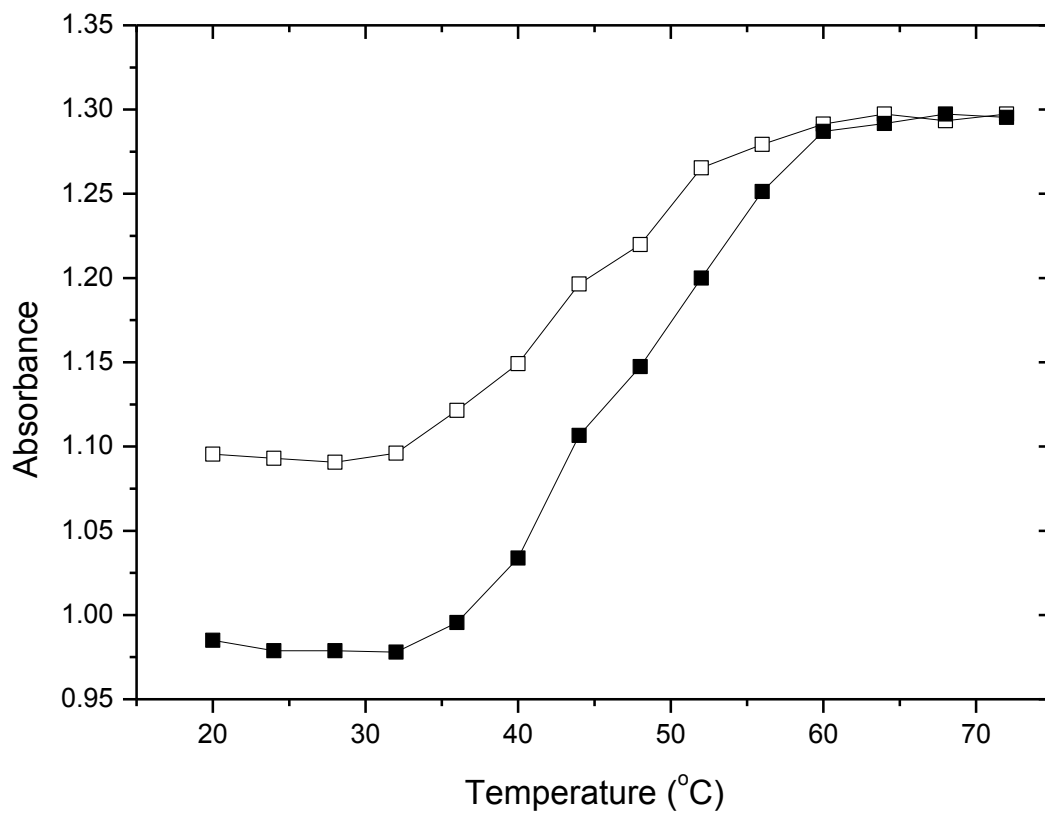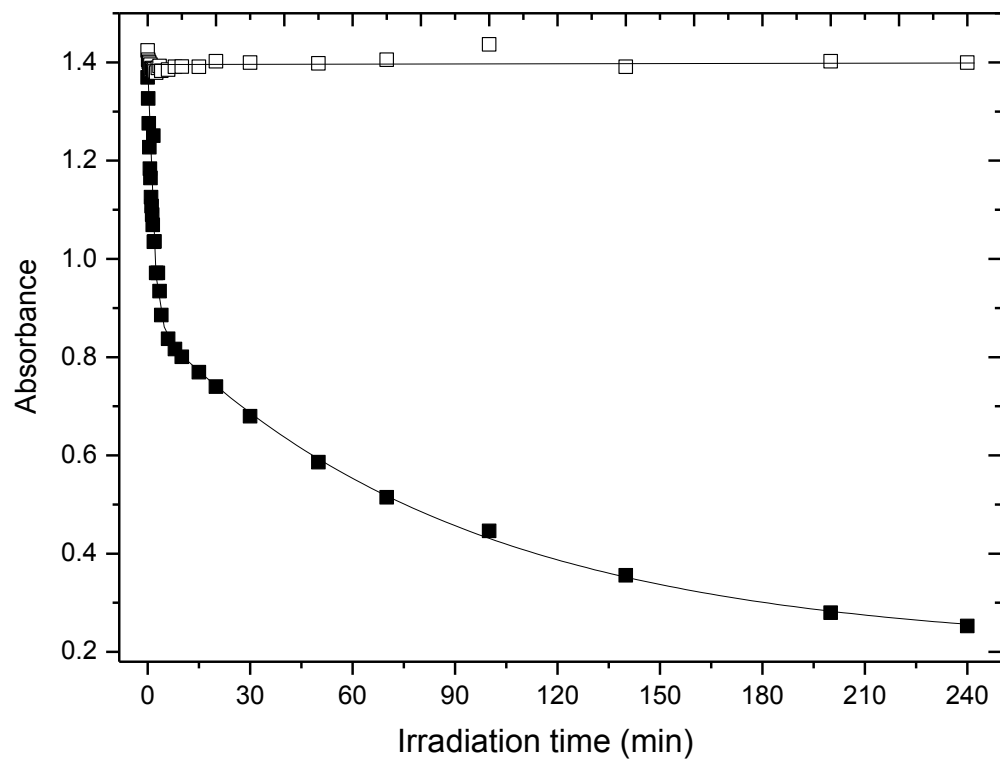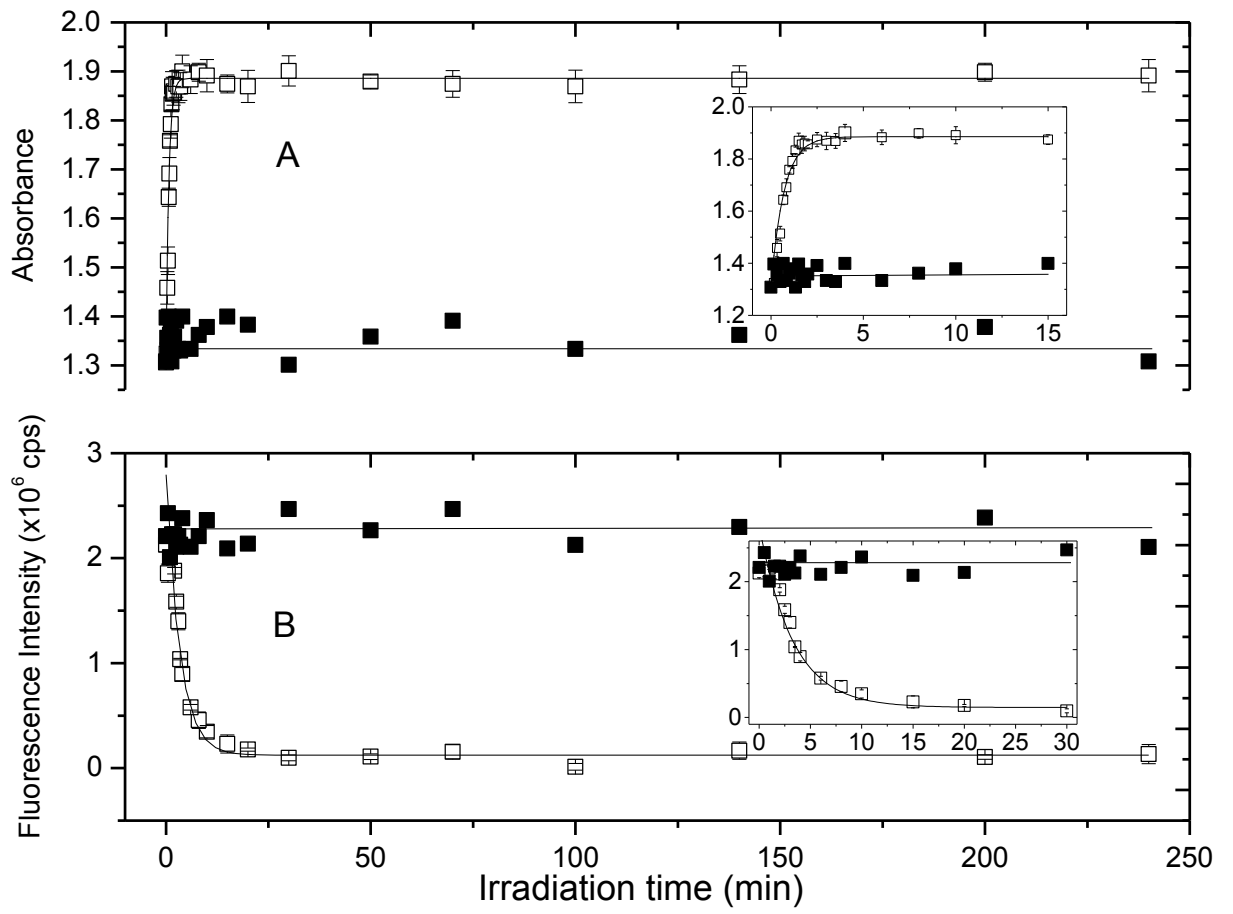measurements. Solutions were measures in 1 cm cuvettes.

Figure 1

Figure 2

Figure 3

Figure 4